

# PCCP

Accepted Manuscript



This is an *Accepted Manuscript*, which has been through the Royal Society of Chemistry peer review process and has been accepted for publication.

*Accepted Manuscripts* are published online shortly after acceptance, before technical editing, formatting and proof reading. Using this free service, authors can make their results available to the community, in citable form, before we publish the edited article. We will replace this *Accepted Manuscript* with the edited and formatted *Advance Article* as soon as it is available.

You can find more information about *Accepted Manuscripts* in the [Information for Authors](#).

Please note that technical editing may introduce minor changes to the text and/or graphics, which may alter content. The journal's standard [Terms & Conditions](#) and the [Ethical guidelines](#) still apply. In no event shall the Royal Society of Chemistry be held responsible for any errors or omissions in this *Accepted Manuscript* or any consequences arising from the use of any information it contains.

## Effects of Constituent Ions of a Phosphonium-based Ionic Liquid on Molecular Organization of H<sub>2</sub>O as Probed by 1-Propanol: Tetrabutylphosphonium and Trifluoroacetate Ions

Takeshi Morita,<sup>\*,a</sup> Kumiko Miki,<sup>b</sup> Ayako Nitta,<sup>a</sup> Hiroyo Ohgi,<sup>a</sup> and Peter Westh<sup>c</sup>

<sup>a</sup> Graduate School of Advanced Integration Science, Chiba University, Chiba 263-8522, Japan

<sup>b</sup> Department of Liberal Arts and Basic Sciences, College of Industrial Technology, Nihon University, Narashino, Chiba 275-8575, Japan

<sup>c</sup> NSM Research for Functional Biomaterials, Roskilde University, Roskilde DK-4000, Denmark

### ABSTRACT

Aqueous solutions of tetrabutylphosphonium trifluoroacetate, [P<sub>4444</sub>]<sup>+</sup>CF<sub>3</sub>COO<sup>-</sup>, exhibit a liquid-liquid phase transition with a lower critical solution temperature. Herein, we characterized the constituent ions, [P<sub>4444</sub>]<sup>+</sup> and CF<sub>3</sub>COO<sup>-</sup>, in terms of their effects on the molecular organization of H<sub>2</sub>O on the basis of 1-propanol probing methodology devised by Koga *et al.* The resulting characterization of the hydrophobicity/hydrophilicity is displayed on a two-dimensional map together with previous results, for a total of four cations and nine anions of typical ionic liquid (IL) constituents. The results indicate that [P<sub>4444</sub>]<sup>+</sup> is the most significant amphiphile with strong hydrophobic and equally strong hydrophilic contributions among the group of constituent cations of ILs studied so far. The hydration number for [P<sub>4444</sub>]<sup>+</sup> was evaluated to be  $n_H = 72$ , which is three times larger than that of a typical imidazolium-based cation, [C<sub>4mim</sub>]<sup>+</sup>. Self-aggregation of [P<sub>4444</sub>]<sup>+</sup> was found to occur in aqueous solution of [P<sub>4444</sub>]<sup>+</sup>CF<sub>3</sub>COO<sup>-</sup> above 0.0080 mole fraction of the IL.

## INTRODUCTION

Ionic liquids (ILs) have gained considerable attention as they have radically changed the concept of the nature of liquids.<sup>1-5</sup> ILs consisting entirely of ions have been increasingly proposed as alternatives to conventional organic solvents. Recent studies have focused on mixed systems composed of ILs and other molecular liquids, rather than neat ILs, for use as functional materials.<sup>6-12</sup> In particular, thermoresponsive phase behaviour of aqueous solutions of ILs has been extensively investigated in relation to phase transitions with lower critical solution temperatures (LCSTs)<sup>6,12,13</sup> as well as upper critical solution temperatures (UCSTs).<sup>13a,13c,13d, 13m,14</sup>

A UCST behaviour is understandable; a strong attraction in terms of enthalpy between species would bring phase separation at low temperatures, while at higher temperatures the total entropic effect drives the system to a random mixture. This transition is caused because the mixing entropic contribution in the mixing Gibbs energy generally becomes more dominant as temperature ( $T$ ) increases. Since the enthalpy-entropy compensation is operative particularly in aqueous solutions, temperature could tip the balance of  $\Delta_{\text{mix}}H$  and  $T\Delta_{\text{mix}}S$  terms, where  $\Delta_{\text{mix}}H$  and  $\Delta_{\text{mix}}S$  are the change of the mixing enthalpy and entropy, respectively. However, an LCST behaviour is not as simple to explain. The present aqueous solution of [P<sub>4444</sub>]CF<sub>3</sub>COO exhibits LCST-type phase behaviour with the critical point at 29.2 °C and 0.025 mole fraction of the IL.<sup>7</sup> The chemical structure of [P<sub>4444</sub>]CF<sub>3</sub>COO is shown in Figure 1.

It has been suggested that LCST behaviour depends on the balance of hydrophilicity and hydrophobicity of the IL constituent ions. Kohno *et al.*<sup>15</sup> reported that LCST-type phase behaviours of aqueous solutions of ILs strongly depend on the “hydrophilicity” of each constituent cation and anion. Their analysis was based on one-dimensional scale with hydrophilicity and hydrophobicity at the extreme ends. The miscibility of imidazolium-based ILs with water was evaluated from estimated partition coefficients in

octanol-water systems.<sup>16,17</sup> The origin of LCST- and UCST-type phase transitions of mixtures of thiophene with two ILs, [C<sub>4</sub>C<sub>1</sub>mim]SCN and [C<sub>4</sub>C<sub>1</sub>mim][NTf<sub>2</sub>], was investigated using NMR spectroscopy and molecular dynamics simulations by Batista *et al.*<sup>18</sup>

Koga *et al.*<sup>19-21</sup> devised a method by which an individual ion can be characterized in terms of a two-dimensional (2D) hydrophilicity and hydrophobicity scale. This technique is known as the 1-propanol (1P)-probing methodology. By this method, “amphiphiles” with hydrophobic and hydrophilic contributions can be quantitatively assessed. Here, we applied this method to characterize the constituent ions of [P<sub>4444</sub>]CF<sub>3</sub>COO to seek a deeper insight.

A differential thermodynamic approach to characterize the effects of a solute on the molecular organization of H<sub>2</sub>O was devised by Koga *et al.*<sup>19</sup> They realized that aqueous solutions consist of three composition regions in each of which the mixing scenario on the molecular level is qualitatively different. The mixing scenario is identified by the term “mixing scheme” instead of solution structure, since the word “structure” implies a stable, ordered molecular arrangement. The mixing schemes are labelled as I, II or III from the H<sub>2</sub>O-rich regions. In Mixing Scheme I, hydrogen bonds of H<sub>2</sub>O are bond-percolated throughout the entire bulk of H<sub>2</sub>O. The transition to Mixing Scheme II from I is regarded as a loss of bond percolation when the hydrogen bond probability is reduced to the percolation threshold. The 1P-probing methodology is applicable only in the region of Mixing Scheme I.

Although the 1P-probing methodology was described in detail elsewhere,<sup>19,20</sup> a brief description is given here. This methodology is based on the finding that, within Mixing Scheme I, the effects of separate solutes on H<sub>2</sub>O are additive.<sup>19</sup> Thus, we study a ternary system, 1P–S–H<sub>2</sub>O, where S is the test sample whose effect on H<sub>2</sub>O is being examined. In the ternary system of 1P–S–H<sub>2</sub>O, the thermodynamic signature of 1P,  $H_{1P}^E$  (defined

below), is evaluated. Modification to its  $x_{1P}$ -dependence pattern due to the presence of S is used to characterize the effect of S on H<sub>2</sub>O.  $H_{1P1P}^E$  is the enthalpic 1P–1P interaction in a complex ternary system and is defined as,

$$H_{1P1P}^E \equiv N (\partial H_{1P}^E / \partial n_{1P}) = (1-x_{1P})(\partial H_{1P}^E / \partial x_{1P}), \quad (1)$$

where

$$H_{1P}^E \equiv (\partial H^E / \partial n_{1P}), \quad (2)$$

and  $H^E$  is the total excess enthalpy in the  $(p, T, n_{1P}, n_S, n_W)$  variable system,  $N = n_{1P} + n_S + n_W$  and  $x_{1P} = n_{1P}/N$ . The subscripts 1P, S and W signify 1-propanol, test sample S and H<sub>2</sub>O, respectively. We directly measure the excess partial molar enthalpy of 1P,  $H_{1P}^E$ . To do so, we perturb the ternary system by increasing  $n_{1P}$  to  $n_{1P} + \delta n_{1P}$ , with a fixed initial mole fraction of S,  $x_S^0 = n_S/(n_S + n_W)$ , and measure the  $H^E$  response,  $\delta H^E$ . We approximate the quotient  $\delta H^E / \delta n_{1P}$  to the partial derivative in Eq. (2), and evaluate  $H_{1P1P}^E$  by differentiating the data set  $(x_{1P}, H_{1P}^E)$  using the far right of Eq. (1).

Figure 2 shows a schematic representation of the changes in the  $H_{1P1P}^E$  pattern induced by the presence of various classes of solute, S. As shown in Figures 2(a)–(d), the peak top is named point X, which marks the end of Mixing Scheme I. Upon addition of S, point X shifts depending on the nature of S. The shifts are in general linear to the initial mole fraction of S,  $x_S^0$ , within Mixing Scheme I. The slope of the westward shift (i.e. to the negative direction of  $x_{1P}$ ) of point X per unit increase in  $x_S^0$  is taken as the *hydrophobicity index*, while that towards the south (i.e. to the negative direction of the  $H_{1P1P}^E$  axis) is the *hydrophilicity index*.

Figure 2(a) shows a typical change in  $H_{1P1P}^E$  for hydration centres such as in  $\text{Na}^+$  and  $\text{Cl}^-$  ion pairs.<sup>22,23</sup> On addition of the salt, the  $H_{1P1P}^E$  pattern is compressed to the west. This compression indicates that, on addition of the  $\text{Na}^+$  and  $\text{Cl}^-$  ion pair, the available  $\text{H}_2\text{O}$  molecules for 1P to interact with are reduced. We thus interpret this westward shift to be due to hydration of the ions. From the westward shift of point X as a function of  $x_S^0$ , the hydration number,  $n_H$ , can be evaluated for  $\text{Na}^+$  and  $\text{Cl}^-$ . It must be stressed that at the starting point,  $x_{1P} = 0$ , the value of  $H_{1P1P}^E$  remains the same even in the presence of  $\text{Na}^+$  and  $\text{Cl}^-$ . This invariance and the fact that the value of  $H_{1P1P}^E$  at point X also remains the same led to the following suggestions: (1)  $\text{Na}^+$  and  $\text{Cl}^-$  ions are hydrated by a number of  $\text{H}_2\text{O}$  molecules, (2) the hydrating  $\text{H}_2\text{O}$  molecules are unavailable to interact with 1P and (3) the bulk  $\text{H}_2\text{O}$  molecules away from the hydration shells are unperturbed by  $\text{Na}^+$  and  $\text{Cl}^-$  even in the presence of the ions. This finding can be utilized to characterize individual ions. For a given test ion, we chose the counter ion  $\text{Na}^+$  or  $\text{Cl}^-$  and applied the 1P probing on the combined salt. Namely, we used tetrabutylphosphonium chloride,  $[\text{P}_{4444}]\text{Cl}$ , and sodium trifluoroacetate,  $\text{NaCF}_3\text{COO}$ , to characterize  $[\text{P}_{4444}]^+$  and  $\text{CF}_3\text{COO}^-$ , respectively.

Figure 2(b) shows the behaviour of the hydrophobic solute. For a solute almost equally hydrophobic as 1P such as 2-propanol<sup>24</sup> the  $H_{1P1P}^E$  pattern shifts parallel to the west, as shown in the figure. This parallel shift is expected when compared to the case in which 1P was added as S to  $x_S^0$  (i.e.  $S = 1P$ ). For a hydrophobe that is stronger (or weaker) than the probing 1P, such as *tert*-butanol<sup>25</sup> (or ethanol<sup>26</sup>), the westward shift is greater (or lesser), reflecting a larger (or smaller)  $n_H$ . This westward shift of point X indicates that a hydrophobe is hydrated by  $\text{H}_2\text{O}$  molecules, making them unavailable to interact with 1P, as

was the case for the hydration centre. In addition, the value of  $H_{1P1P}^E$  at point X shifts northward (or southward), reflecting the fact that the ability of *tert*-butanol (or ethanol) to reduce the hydrogen bond probability of bulk H<sub>2</sub>O away from hydration shell is greater (or lesser) than 1P, as studied earlier.<sup>19</sup> Furthermore, the hydrogen bondings within the hydration shells are more organized than it is in bulk H<sub>2</sub>O.

Figure 2(c) is the pattern change for the hydrophilic solute. This finding, as well as others,<sup>19</sup> led to the interpretation that hydrophiles form hydrogen bonds directly to the existing hydrogen bond network of H<sub>2</sub>O and maintain the hydrogen bond connectivity of the network; thus, they act as impurities in the network. As such, they break the H donor/acceptor symmetry. Hence, the southward shift apparent in the figure is interpreted as a reduction of the net entropy-volume cross fluctuation.

Figure 2(d) is for the amphiphilic solute. The effects seem to be a combination of those observed for hydrophobic and hydrophilic moieties. Their westward and southward components show contributions from hydrophobic and hydrophilic moieties, respectively. Typical IL constituent ions generally show amphiphilic responses to 1P-probing studies with strong hydrophobic and equally strong hydrophilic characteristics.<sup>27–30</sup> These results fit into the special properties of ILs. Low melting points for ionic compounds can be related to the strength of hydrophobicity and/or hydrophilicity.<sup>20,30</sup>

With this pair of coordinates, the characterization of each species, including individual constituent ions, is displayed on a 2D map of hydrophobicity/hydrophilicity.

## EXPERIMENTAL

### Titration calorimetry for 1P probing

Tetrabutylphosphonium chloride,  $[P_{4444}]Cl$ , (Aldrich, >98%) was used as the sample for characterization of the cation,  $[P_{4444}]^+$ . Sodium trifluoroacetate,  $NaCF_3COO$ , (Sigma-Aldrich, >96%) was used as the sample for that of  $CF_3COO^-$ . Deionized  $H_2O$  was prepared using a Milli-Q system (Millipore), with a resulting resistivity of  $18.2\text{ M}\Omega\cdot\text{cm}$ . Stock solutions were prepared using the purified  $H_2O$  and the salts from freshly opened bottles. 1-Propanol (1P) (Sigma-Aldrich, Chromasolv for HPLC 99.9+%) was used as supplied. Due care was exercised not to contaminate the 1P with moisture from the atmosphere. The excess partial molar enthalpy,  $H_{1P}^E$ , was determined using a TAM III semi-isothermal titration calorimeter (TA Instruments, New Castle, USA) at  $25.0\text{ }^\circ\text{C} \pm 0.0001\text{ }^\circ\text{C}$  and in the dynamic correction mode.<sup>31-33</sup> A 1 mL stainless steel container was used as the cell. The initial volume of the sample solution was set at  $750\text{ }\mu\text{L}$  and the exact amount was determined gravimetrically. The volume and duration of each titration of 1P were set at  $10\text{ }\mu\text{L}$  and  $10\text{ s}$ , respectively. The injection volume per titration was calibrated to  $9.9483\text{ }\mu\text{L}$  and was used to calculate the concentration. The ratio of titrant over titrand was on the order of  $10^{-2}$  and was well within the acceptable range for approximation of the differentiation. The interval of injection was set at  $30\text{ min}$ . The averaged uncertainty of the titration measurements was estimated to be  $\pm 0.03\text{ kJ mol}^{-1}$ .

### Electric conductivity

The IL,  $[P_{4444}]CF_3COO$ , was synthesized and used for conductivity measurements. It was prepared by direct neutralization of aqueous tetrabutylphosphonium hydroxide solutions with trifluoroacetic acid. After evaporation, the product was added to a dichloromethane/water biphasic system and the resulting mixture was washed several times with distilled water. The required  $[P_{4444}]CF_3COO$  was dissolved in dichloromethane phase,

and was dried in vacuum for 24 h at 60 °C prior to use. The structure and purity were confirmed by  $^1\text{H}$  NMR spectroscopy. The procedure of the synthesis has been described elsewhere in detail.<sup>7</sup>

The electric conductivity of the aqueous solution was measured using an electrical conduction metre with automatic temperature compensation (Hanna instruments, DiST4). The measured concentration range was from a 0.001127 to 0.04610 mole fraction of the IL.

## RESULTS AND DISCUSSION

The data of  $H_{1\text{P}}^{\text{E}}$  are deposited as Table S1 of the Supporting Information and are plotted in Figure 3. A sigmoidal increase in  $H_{1\text{P}}^{\text{E}}$  with an inflection point is evident as long as  $x_{\text{S}}^0$  is appropriate for performing the 1P-probing methodology. As shown in Figure 3, the  $x_{1\text{P}}$ -dependence pattern of  $H_{1\text{P}}^{\text{E}}$  changes more rapidly for  $\text{S} = [\text{P}_{4444}]\text{Cl}$  with increasing  $x_{\text{S}}^0$  than it does for  $\text{S} = \text{NaCF}_3\text{COO}$ . The inflection point seems to disappear at  $x_{\text{S}}^0 = 0.011$  for  $\text{S} = [\text{P}_{4444}]\text{Cl}$  and at  $x_{\text{S}}^0 = 0.055$  for  $\text{S} = \text{NaCF}_3\text{COO}$ . To see this behaviour more clearly, we took the derivative of  $H_{1\text{P}}^{\text{E}}$  with respect to  $x_{1\text{P}}$ .

### Evaluation of $H_{1\text{P}1\text{P}}^{\text{E}}$ from $H_{1\text{P}}^{\text{E}}$ data

With a good set of raw  $H_{1\text{P}}^{\text{E}}$  data with an averaged uncertainty of  $\pm 0.03 \text{ kJ mol}^{-1}$  and small increments in  $x_{1\text{P}}$ , the raw  $H_{1\text{P}}^{\text{E}}$  data themselves were used to calculate the derivative on the far right of Eq. (1). In general, numerical derivative directly using two neighbouring data points causes large noise, especially in applications with raw experimental data. In the present study, we originally utilized a differential method based on Eq. (3) for calculation of

the partial molar quantities with higher-order derivatives. We approximate the slope of the tangent at the  $i$ -th point as the weighted average of the slopes of the two adjacent arcs; one between the  $(i-1)$ -th and  $i$ -th data points and another between the  $i$ -th and  $(i+1)$ -th data points.

$$\begin{aligned}
 H_{1P1P}^E(i) &= \{1 - x_{1P}(i)\} \left\{ \frac{\partial H_{1P}^E(i)}{\partial x_{1P}(i)} \right\} \\
 &\approx \frac{\{1 - x_{1P}(i)\}}{\{x_{1P}(i+1) - x_{1P}(i-1)\}} \left[ \frac{\{H_{1P}^E(i+1) - H_{1P}^E(i)\}}{\{x_{1P}(i+1) - x_{1P}(i)\}} \{x_{1P}(i) - x_{1P}(i-1)\} \right. \\
 &\quad \left. + \frac{\{H_{1P}^E(i) - H_{1P}^E(i-1)\}}{\{x_{1P}(i) - x_{1P}(i-1)\}} \{x_{1P}(i+1) - x_{1P}(i)\} \right] \quad (3)
 \end{aligned}$$

The  $x_{1P}$  interval of  $x_{1P}(i)$  to  $x_{1P}(i+1)$ ,  $\delta x_{1P}$ , was approximately 0.003 in the present measurements. It is found that  $\delta x_{1P} \approx 0.008$  in graphical evaluation normally exercised is appropriate to approximate the derivative of Eq. (1) with the quotient  $\delta H_{1P}^E / \delta n_{1P}$ .<sup>34</sup> In the present calculations, the total  $\delta x_{1P}$  for three neighbouring data points was approximately 0.006.

Certainty in evaluation of the partial molar quantities with higher-order derivatives is of particular importance in the present study. Figures 4(a)–(c) show comparisons of  $H_{1P1P}^E$  determined using Eq. (3) and that determined using other evaluation methods. Figure 4(a) shows comparison between the  $H_{1P1P}^E$  pattern obtained using Eq. (3) and that evaluated by the graphical method normally exercised. As shown in Figure 4(b), combination of Eq. (3) and the graphical evaluation shows improvement especially in the pre-peak region. The point X evaluated by the  $H_{1P1P}^E$  pattern corresponds to each other regardless of the method. Figure 4(c) shows comparison between Eq.(3) and simple derivative using two neighbouring data

points. As mentioned above, the calculation using Eq. (3) is superior to the simple derivative using two alternating data points with regard to noise reduction, as shown in Figure 4(c). Therefore, it is concluded that the calculation based on Eq. (3) is the most certain for evaluation of partial molar quantities with higher-order derivatives in the present data set. Thus, calculation based on Eq. (3) was utilized here for evaluation of  $H_{IP1P}^E$ , leading to determination of the hydrophobicity and hydrophilicity indices.

### Hydrophobicity/hydrophilicity obtained from $H_{IP1P}^E$ pattern

Figures 5 and 6 show the patterns of resulting  $H_{IP1P}^E$  for  $S = [P_{4444}]Cl$  and  $S = NaCF_3COO$ , respectively. The peak top of  $H_{IP1P}^E$  appears at 0.049 of  $x_{1P}$  for binary (1-propanol–H<sub>2</sub>O) mixture.<sup>19</sup> The peak top shifts to the west (direction of smaller  $x_{1P}$ ) as  $x_S^0$  increases. Point X nearly disappears at  $x_S^0 = 0.0110$  for  $S = [P_{4444}]Cl$  and  $x_S^0 = 0.0550$  for  $S = NaCF_3COO$ , qualitatively indicating that the hydrophobicity of  $[P_{4444}]Cl$  is much larger than that of  $NaCF_3COO$ . The starting point of  $H_{IP1P}^E$  at  $x_{1P} = 0$  shifts to the north (direction of larger  $H_{IP1P}^E$ ) with increasing  $x_S^0$ . This northward shift also corresponds to the strong hydrophobicity of  $[P_{4444}]^+$ . For  $NaCF_3COO$ , the equivalent shift at  $x_{1P} = 0$  is lesser.

The degrees of the shifts are plotted in Figures 7 and 8. The slopes of  $x_{1P}$  loci shown in Figures 7(a) and 8(a) yielded the hydrophobicity indices and hydration numbers,  $n_H$ . The contribution from counter ions ( $Na^+$  or  $Cl^-$ ) was corrected by subtraction in the evaluation. The slopes of the  $H_{IP1P}^E$  loci in Figures 7(b) and 8(b) directly correspond to the hydrophilicity indices in the present evaluation. The hydrophilicity indices of the counter ions of  $Na^+$  and  $Cl^-$  used in the present study are equal to zero, since these ions are classified

as hydration centre. As mentioned in Introduction, hydration centres such as  $\text{Na}^+$  and  $\text{Cl}^-$  unperturb the bulk  $\text{H}_2\text{O}$  molecules away from the hydration shells around the ions. Hydrophobicity/hydrophilicity indices and hydration numbers of  $[\text{P}_{4444}]^+$  and  $\text{CF}_3\text{COO}^-$  are listed in Table 1.

The results indicate that  $[\text{P}_{4444}]^+$  is an amphiphile with strong hydrophobic and equally strong hydrophilic contributions.  $[\text{P}_{4444}]^+$  forms a large hydration shell with a hydration number of  $n_{\text{H}} = 72$ , which is three times larger than that of typical imidazolium-based cation 1-butyl-3-methylimidazolium,  $[\text{C}_4\text{mim}]^+$ .<sup>27</sup> The value of a hydration number for  $\text{CF}_3\text{COO}^-$  was found to be  $n_{\text{H}} = 10$ . On the basis of earlier findings in 1P-probing studies on a series of carboxylates,<sup>36</sup> one  $\text{H}_2\text{O}$  molecule out of the 10  $\text{H}_2\text{O}$  molecules should be used for hydration of the  $-\text{COO}^-$  side and the remaining 9.0  $\text{H}_2\text{O}$  molecules for the fluoroalkyl group,  $-\text{CF}_3$ . This hydration number is much larger than that of the alkyl group in  $\text{CH}_3\text{COO}^-$ ; the hydration number for  $-\text{CH}_3$  in  $\text{CH}_3\text{COO}^-$  is estimated to be 2.7.<sup>36</sup> The fact that the fluoroalkyl group is a stronger hydrophobe than the alkyl group could be related to this finding,<sup>37</sup> an aqueous solution of the  $\text{CF}_3\text{COO}^-$  salt of  $[\text{P}_{4444}]^+$  shows LCST, and that of the  $\text{CH}_3\text{COO}^-$  salt does not.

### Self-aggregation behaviour of $[\text{P}_{4444}]^+$

As shown in Figure 7, the induced changes at  $x_{\text{S}}^0 = 0.010$  for  $\text{S} = [\text{P}_{4444}]\text{Cl}$  depart from the linear relationship defined in the lower  $x_{\text{S}}^0$  region. This departure shifts to the upper side beyond the data error in the present evaluation. This departure hints the self-aggregation of the kind found in imidazolium-based ILs. For  $[\text{C}_4\text{C}_1\text{mim}]\text{Cl}$ <sup>29</sup> and  $[\text{C}_4\text{mim}]\text{Cl}$ <sup>27</sup>, similar plots are seen that show a break in the slopes at  $x_{\text{S}}^0 = 0.006$  and 0.014, respectively. For aqueous solutions of  $[\text{C}_4\text{mim}]\text{BF}_4$ , this similar behaviour was interpreted as self-aggregation of

cations through NMR spectroscopy,<sup>38</sup> electric conductivity,<sup>39,40,41</sup> small-angle neutron scattering,<sup>41,42</sup> density,<sup>43</sup> speed of sound<sup>43</sup> and surface tension.<sup>39,41</sup> Thus, we suggest that departure of the induced change at  $x_S^0 = 0.010$  for the case shown in Figure 7 could also be caused by self-aggregation of  $[P_{4444}]^+$ .

For further investigation of this issue, electric conductivity measurements were conducted for the aqueous solutions of  $[P_{4444}]CF_3COO$ . The obtained conductivity was converted to molar conductivity according to the Kohlrausch empirical relation.<sup>42</sup> Figure 9 shows the isotherm of the molar conductivity as a function of the square root of IL concentration. The linear portion represents the usual behaviour of ionic solutions in the dilute region. This linearity seems to start to deviate at  $\sqrt{c} = 19.6 \text{ (mmol}\cdot\text{L}^{-1})^{1/2}$ , which corresponds to a mole fraction of 0.0080. The fact that the conductivity shows deviation from the usual behaviour at  $x_{IL} = 0.0080$  suggests that  $[P_{4444}]CF_3COO$  dissociates into its constituent ions in the dilute region and aggregation of  $[P_{4444}]^+$  begins at a mole fraction of approximately 0.0080, as the case for imidazolium-based ILs. Considering the larger hydrophobicity (hydration number) of  $[P_{4444}]^+$  compared to those of  $[C_4mim]^+$  and  $[C_4C_1mim]^+$ , the breakpoint (or aggregation) of  $[P_{4444}]^+$  might be expected at a much lower concentration; however, this was not observed. This discrepancy could be related to the difference in the aggregation mechanisms of imidazolium-based and phosphonium-based cations. The imidazolium ions have an ionic head and alkyl tail, while phosphonium-based ions have an ionic centre and four alkyl tails extending in random directions. Wang *et al.* suggested that the aggregation aspect of  $[P_{4444}]CF_3COO$  in aqueous solution can be described in terms of microemulsion-like aggregation at the mesoscale level in higher concentration ranges near the critical point.<sup>45</sup>

## 2D map of hydrophobicity/hydrophilicity

Figure 10 shows the 2D map of hydrophobicity/hydrophilicity for  $[P_{4444}]^+$  and  $CF_3COO^-$ . In the map,  $H_2O$  defines the origin (0,0). 1-Propanol used as the probe is necessarily plotted at (-1,0). Relative to these points, ions with greater hydrophobic contributions spread to the west (negative horizontal direction) and those with greater hydrophilic contributions spread to the south (negative vertical direction). A total of four cations and nine anions of typical IL constituents are plotted in Figure 10. The cations<sup>20,21</sup> are  $[C_2mim]^+$ ,  $[C_4mim]^+$ ,  $[C_4C_1mim]^+$  and the present  $[P_{4444}]^+$ . The anions<sup>20,21,30</sup> are  $Cl^-$ ,  $CH_3COO^-$ ,  $Br^-$ ,  $BF_4^-$ ,  $[OTf]^-$ ,  $PF_6^-$ ,  $[NTf_2]^-$  and the present  $CF_3COO^-$ . As evident from Figure 10,  $[P_{4444}]^+$  shows the most significant amphiphilicity, with strong hydrophobic and equally strong hydrophilic contributions, among the constituent cations of the ILs studied. Furthermore, the IL constituent ions are located farther from the origin than are the typical inorganic small ions. Our recent study on normal ions (i.e. non-IL forming ions) shows that anions are located farther from the origin than cations.<sup>46</sup>

Kohno *et al.*<sup>15</sup> took advantage of the phase separation of IL- $H_2O$  systems and estimated the  $H_2O$  content in the IL phase. They then determined the hydration number per mole of IL and defined it as the hydrophilicity of the IL. They concluded that the LCST behaviour strongly depended on the evaluated “hydrophilicity” indices. We point out that their hydrophilicity concept is based on the  $H_2O$  content in the IL-rich situation. In the 1P probing, hydrophilicity is only a part of the effects of the ion in question to  $H_2O$  in the water-rich region, the other part being hydrophobicity. Saita *et al.*<sup>47</sup> suggested another one-dimensional scale based on salt effects of test ions fixed as  $[P_{4444}]^+$  or  $CF_3COO^-$  counter ion on the LCST of  $[P_{4444}]CF_3COO-H_2O$  system. It is concluded that changes in the critical temperatures of IL- $H_2O$  systems are clearly related to the “hydrophilicity” of the target ions.

In the present 1P-probing methodology, the hydration number of the species in question

is evaluated from “hydrophobicity” index. The hydrophobicity is defined on the basis of hydration of the solute with H<sub>2</sub>O molecules, namely the formation of the hydration shell in water-rich region. Hydrophile in the 1P probing is defined as a solute that forms hydrogen bonds directly to the existing hydrogen bond network of H<sub>2</sub>O, discussed in detail in Introduction. As shown in Figure 10, the typical constituent ions are classified as “amphiphiles” with strong hydrophobic and equally strong hydrophilic contributions. Thus, the present two-dimensional scale covers the ranking of “hydrophilicity” from the one-dimensional scale and might lead to a deeper understanding on the effects of molecular organization of H<sub>2</sub>O.

## Conclusions

The constituent ions of [P<sub>4444</sub>]CF<sub>3</sub>COO were characterized in terms of their effects on the molecular organization of H<sub>2</sub>O using the 1P-probing methodology. A differential method based on the weighted average of two slopes was utilized to calculate  $H_{1P1P}^E$ . The most significant amphiphile among the IL constituent cations studied was [P<sub>4444</sub>]<sup>+</sup>, which had strong hydrophobic and equally strong hydrophilic contributions. The hydration number was evaluated to be  $n_H = 72$ , which was the largest value among the group of cations. Characterization of CF<sub>3</sub>COO<sup>-</sup> clarified that it was a hydrophobe with a hydration number of  $n_H = 10$ , out of which one H<sub>2</sub>O molecule hydrated the –COO<sup>-</sup> side and the remaining 9.0 H<sub>2</sub>O molecules the fluoroalkyl group, –CF<sub>3</sub>. The self-aggregation behaviour of [P<sub>4444</sub>]<sup>+</sup> in the aqueous solution of [P<sub>4444</sub>]CF<sub>3</sub>COO was revealed above 0.0080 mole fraction of the IL.

It is suggested that the formation of the large hydration shell around [P<sub>4444</sub>]<sup>+</sup> evaluated in the present study causes loss in excess entropy of mixing. Hence, this entropic loss must have bearing to the present LCST behaviour as mentioned in Introduction. Koga *et al.* sorted

out the occurrence of phase separation with an LCST as well as a UCST in terms of signs of  $H_{ii}^E$  and  $S_{ii}^E$ , the third derivative of  $G^E$  in binary solute(i)–H<sub>2</sub>O system.<sup>19,48</sup> Although their argument was based on a necessary but not sufficient condition, it was applied to [C<sub>4</sub>mim]BF<sub>4</sub>–H<sub>2</sub>O system and the  $H_{ii}^E$  and  $S_{ii}^E$  for  $i = [\text{C}_4\text{mim}]\text{BF}_4$  was found to be negative, which is appropriate for the UCST at 4 °C and  $x_i = 0.07$ .<sup>49</sup> For the present case, however, since we have not yet determined  $H_i^E$  and  $S_i^E$  for  $i = [\text{P}_{4444}]\text{CF}_3\text{COO}$ , we will postpone the detailed discussions about the occurrence of LCST for aqueous solution of the present IL. As shown in Figure 10, 2-butoxyethanol (BE) was found to form an analogously large hydration shell around the molecule,  $n_H = 58$ ,<sup>23</sup> and the aqueous solution of BE exhibits the LCST below 50 °C.<sup>50,51</sup>

### Acknowledgements

We would like to express the deepest appreciation to Dr. Y. Koga at the University of British Columbia for his discussion about the 1P-probing experiment and critical reading of the manuscript. We are deeply grateful to Prof. H. Ohno, Dr. Y. Kohno and Dr. S. Saita at Tokyo University of Agriculture and Technology for preparation of the ionic liquid used in this study, measurements of the electric conductivity and fruitful discussion. T.M. is grateful to Prof. K. Nishikawa for cooperation of the experiment. This work was partially supported by Grant-in-Aid for Scientific Research (JSPS KAKENHI) (No. 24550009). T.M. thanks MEXT, Japan, for Grants for Excellent Graduate Schools for the financial support for his stay at Roskilde University.

## Notes and references

- 1 J. S. Wilkes and M. J. Zaworotko, *J. Chem. Soc., Chem. Commun.*, 1992, 965.
- 2 T. Welton, *Chem. Rev.*, 1999, **99**, 2071.
- 3 J. F. Wishart and E. W. Castner, Jr., Eds. “*The Physical Chemistry of Ionic Liquids*” (Editorial for Special Issue), *J. Phys. Chem. B*, 2007, **111**, 4639.
- 4 N. V. Plechkova and K. R. Seddon, *Chem. Soc. Rev.*, 2008, **37**, 123.
- 5 P. Wasserscheid and T. Welton, *Ionic Liquids in Synthesis*, 2nd edn, Wiley-VCH, Weinheim, 2008.
- 6 K. Fukumoto and H. Ohno, *Angew. Chem. Int. Ed.*, 2007, **46**, 1852.
- 7 Y. Kohno, H. Arai, S. Saita and H. Ohno, *Aust. J. Chem.*, 2011, **64**, 1560.
- 8 Y. Kohno and H. Ohno, *Chem. Commun.*, 2012, **48**, 7119.
- 9 T. V. Hoogerstraete, B. Onghena, and K. Binnemans, *J. Phys. Chem. Lett.* 2013, **4**, 1659.
- 10 A. J. L. Costa, M. R. C. Soromenho, K. Shimizu, J. M. S. S. Esperança, J. N. C. Lopes and L. P. N. Rebelo, *RSC Adv.*, 2013, **3**, 10262.
- 11 W. Li and P. Wu, *Polym. Chem.*, 2014, **5**, 5578.
- 12 Y. Kohno, S. Saita, Y. Men, J. Yuan and H. Ohno, *Polym. Chem.*, 2015, **6**, 2163.
- 13 (a) H. Glasbrenner and H. Weingärtner, *J. Phys. Chem.*, 1989, **93**, 3378. (b) S. A. Buckingham, C. J. Garvey and G. G. Warr, *J. Phys. Chem.*, 1993, **97**, 10236. (c) H. Weingärtner, M. Kleemeier, S. Wiegand and W. Schröer, *J. Stat. Phys.*, 1995, **78**, 169. (d) M. Kleemeier, W. Schröer and H. Weingärtner, *J. Mol. Liq.*, 1997, **73–74**, 501. (e) Z.-L. Xie and A. Taubert, *Chem. Phys. Chem.*, 2011, **12**, 364. (f) Y. Kohno and H. Ohno, *Aust. J. Chem.*, 2012, **65**, 91. (g) Y. Kohno, Y. Deguchi and H. Ohno, *Chem. Commun.*, 2012, **48**, 11883. (h) S. Saita, Y. Kohno, N. Nakamura and H. Ohno, *Chem. Commun.*, 2013, **49**, 8988. (i) Y. Tsuji and H. Ohno, *Chem. Lett.*, 2013,

- 42, 527. (j) T. Ando, Y. Kohno, N. Nakamura and H. Ohno, *Chem. Commun.*, 2013, **49**, 10248. (k) Y. Fukaya and H. Ohno, *Phys. Chem. Chem. Phys.*, 2013, **15**, 4066. (l) Y. Fukaya and H. Ohno, *Phys. Chem. Chem. Phys.*, 2013, **15**, 14941. (m) S. Saita, Y. Mieno, Y. Kohno and H. Ohno, *Chem. Commun.*, 2014, **50**, 15450. (n) Y. Deguchi, Y. Kohno and H. Ohno, *Chem. Lett.*, 2015, **44**, 238.
- 14 (a) J. E. L. Dullius, P. A. Z. Suarez, S. Einloft, R. F. de Souza and J. Dupont, *Organometallics*, 1998, **17**, 815. (b) P. J. Dyson, D. J. Ellis and T. Welton, *Can. J. Chem.*, 2001, **79**, 705. (c) C. A. Cerdeiriña, J. Troncoso, C. P. Ramos, L. Romani, V. Najdanovic-Visak, H. J. R. Guedes, J. M. S. S. Esperança, Z. P. Visak, M. Nunes da Ponte and L. P. N. Rebelo, in *Ionic Liquids III A: Fundamentals, Progress, Challenges, and Opportunities*, ed. R. Rogers and K. R. Seddon, ACS Symp. Ser., 2005, ch. 13, vol. 901, pp. 175. (d) P. Nockemann, B. Thijs, S. Pittois, J. Thoen, C. Glorieux, K. V. Hecke, L. V. Meervelt, B. Kirchner and K. Binnemans, *J. Phys. Chem. B*, 2006, **110**, 20978. (e) Y. Fukaya, K. Sekikawa, K. Murata, N. Nakamura and H. Ohno, *Chem. Commun.*, 2007, 3089. (f) P. Nockemann, K. Binnemans, B. Thijs, T. N. Parac-Vogt, K. Merz, A.-V. Mudring, P. C. Menon, R. N. Rajesh, G. Cordoyiannis, J. Thoen, J. Leys and C. Glorieux, *J. Phys. Chem. B*, 2009, **113**, 1429.
- 15 Y. Kohno and H. Ohno, *Phys. Chem. Chem. Phys.*, 2012, **14**, 5063.
- 16 U. Doman' ska, E. Bogel-Lukasik and R. Bogel-Lukasik, *Chem.–Eur. J.*, 2003, **9**, 3033.
- 17 L. Ropel, L. S. Belve` ze, S. N. V. K. Aki, M. A. Stadtherr and J. F. Brennecke, *Green Chem.*, 2005, **7**, 83.
- 18 M. L. S. Batista, L. I. N. Tomé, C. M. S. S. Neves, E. M. Rocha, J. R. B. Gomes and J. A. P. Coutinho, *J. Phys. Chem. B*, 2012, **116**, 5985.
- 19 Y. Koga, *Solution Thermodynamics and Its Application to Aqueous Solutions: A Differential Approach*; Elsevier: Amsterdam, 2007 and references are cited in this

textbook.

- 20 Y. Koga, *Phys. Chem. Chem. Phys.*, 2013, **15**, 14548.
- 21 Y. Koga, *J. Mol. Liq.* (in press). doi: 10.1016/j.molliq.2014.09.048.
- 22 P. Westh, H. Kato, K. Nishikawa and Y. Koga, *J. Phys. Chem. A*, 2006, **110**, 2072.
- 23 Y. Koga, P. Westh, K. Nishikawa and S. Subramanian, *J. Phys. Chem. B*, 2011, **115**, 2995.
- 24 J. Hu, W. M. Chiang, P. Westh, D. H. C. Chen, C. A. Haynes and Y. Koga, *Bull. Chem. Soc. Jpn.*, 2001, **74**, 809.
- 25 K. Miki, P. Westh and Y. Koga, *J. Phys. Chem. B*, 2005, **109**, 19536.
- 26 T. Morita, P. Westh, K. Nishikawa and Y. Koga, *J. Phys. Chem. B*, 2012, **116**, 7328.
- 27 K. Miki, P. Westh, K. Nishikawa and Y. Koga, *J. Phys. Chem. B*, 2005, **109**, 9014.
- 28 H. Kato, K. Nishikawa and Y. Koga, *J. Phys. Chem. B*, 2008, **112**, 2655.
- 29 H. Kato, K. Miki, T. Mukai, K. Nishikawa and Y. Koga, *J. Phys. Chem. B*, 2009, **113**, 14754.
- 30 T. Morita, A. Nitta, K. Nishikawa, P. Westh and Y. Koga, *J. Mol. Liq.*, 2014, **198**, 211.
- 31 E. Calvet and H. Prat, *Recent Progress in Microcalorimetry*, Pergamon Press, Oxford, 1963.
- 32 K. R. Loblich, *Thermochim. Acta*, 1994, **231**, 7.
- 33 B. Löwen, S. Schulz and J. Seippel, *Thermochim. Acta*, 1994, **235**, 147.
- 34 M. T. Parsons, P. Westh, J. V. Davies, Ch. Trandum, W. M. Chiang, E. G. M. Yee and Y. Koga, *J. Solution Chem.* 2001, **30**, 1007.
- 35 I. Wadso and R. N. Goldberg, *Pure Appl. Chem.*, 2001, **73**, 1625.
- 36 T. Kondo, Y. Miyazaki, A. Inaba and Y. Koga, *J. Phys. Chem. B*, 2012, **116**, 3571.

- 37 private communication.
- 38 T. Singh and A. Kumar, *J. Phys. Chem. B*, 2007, **111**, 7843.
- 39 J. Bowers, C. P. Butts, P. J. Martin, M. C. V.-Gutierrez and R. K. Heenan, *Langmuir*, 2004, **20**, 2191.
- 40 J. Wang, H. Wang, S. Zhang, H. Zhang and Y. Zhao, *J. Phys. Chem. B*, 2007, **111**, 6181.
- 41 N. V. Sastry, N. M. Vaghela, V. K. Aswal, *Fluid Phase Equilibria*, 2012, **327**, 22.
- 42 L. Almásy, M. Turmine and A. Perera, *J. Phys. Chem. B*, 2008, **112**, 2382.
- 43 M. Tariq, F. Moscoso, F. J. Deive, A. Rodriguez, M. A. Sanroman, J. M. S. S. Esperança, J. N. C. Lopes and L. P. N. Rebelo, *J. Chem. Thermodyn.*, 2013, **59**, 43.
- 44 A. G. Avent, P. A. Chaloner, M. P. Day, K. R. Seddon and T. Welton, *J. Chem. Soc., Dalton Trans.* 1994, 3405.
- 45 R. Wang, W. Leng, Y. Gao and L. Yu, *RSC Adv.*, 2014, **4**, 14055.
- 46 T. Morita, P. Westh, K. Nishikawa and Y. Koga, *J. Phys. Chem. B*, 2014, **118**, 8744.
- 47 S. Saita, Y. Kohno and H. Ohno, *Chem. Commun.*, 2013, **49**, 93.
- 48 Y. Koga, *J. Phys. Chem.*, 1996, **100**, 5172.
- 49 H. Katayanagi, K. Nishikawa, H. Shimozaki, K. Miki, P. Westh and Y. Koga, *J. Phys. Chem. B* 2004, **108**, 19451.
- 50 C. M. Ellis, *J. Chem. Education*, 1967, **44**, 405.
- 51 M. D'Angelo, G. Onori and A. Santucci, *Chem. Phys. Lett.*, 1994, **220**, 59.

Table 1 Hydrophobicity/hydrophilicity indices of  $[P_{4444}]^+$  and  $CF_3COO^-$  as probed by 1-propanol.

ion	class	hydrophobicity	$n_H^a$	hydrophilicity (kJ mol <sup>-1</sup> )	applicable $x_S^0$ range	aggregation <sup>b</sup>	ref.
<b>cations</b>							
$[P_{4444}]^+$	amphiphile	-3.49	72	-5337	< 0.012	$x_S^0 > 0.0080$	this work
$[C_2mim]^+$	amphiphile	-0.39	7	-1970	< 0.024	none	20, 21, 29
$[C_4mim]^+$	amphiphile	-1.31	26	-3227	< 0.029	$x_S^0 > 0.013$	20, 21, 27
$[C_4C_1mim]^+$	amphiphile	-1.85	37	-6760	< 0.018	$x_S^0 > 0.0060$	20, 21, 25
<b>anions</b>							
$CF_3COO^-$	hydrophobe	-0.49	10	-767	< 0.055	none	this work
$CH_3COO^-$	hydrophobe	-0.22	3.7	0	< 0.05	none	20, 21, 36

<sup>a</sup> Hydration number evaluated from the loci of point X.

<sup>b</sup> Aggregation observed in the region of Mixing Scheme I.

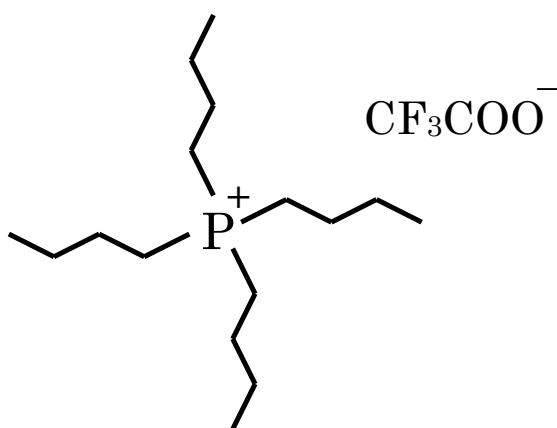


Figure 1 Chemical structure of tetrabutylphosphonium trifluoroacetate, [P<sub>4444</sub>]<sup>+</sup>CF<sub>3</sub>COO<sup>-</sup>. Aqueous solution of the IL exhibits an LCST-type phase transition. In the present study, [P<sub>4444</sub>]<sup>+</sup>Cl<sup>-</sup> and NaCF<sub>3</sub>COO were used for characterization of the individual constituent ions, [P<sub>4444</sub>]<sup>+</sup> and CF<sub>3</sub>COO<sup>-</sup>, respectively.

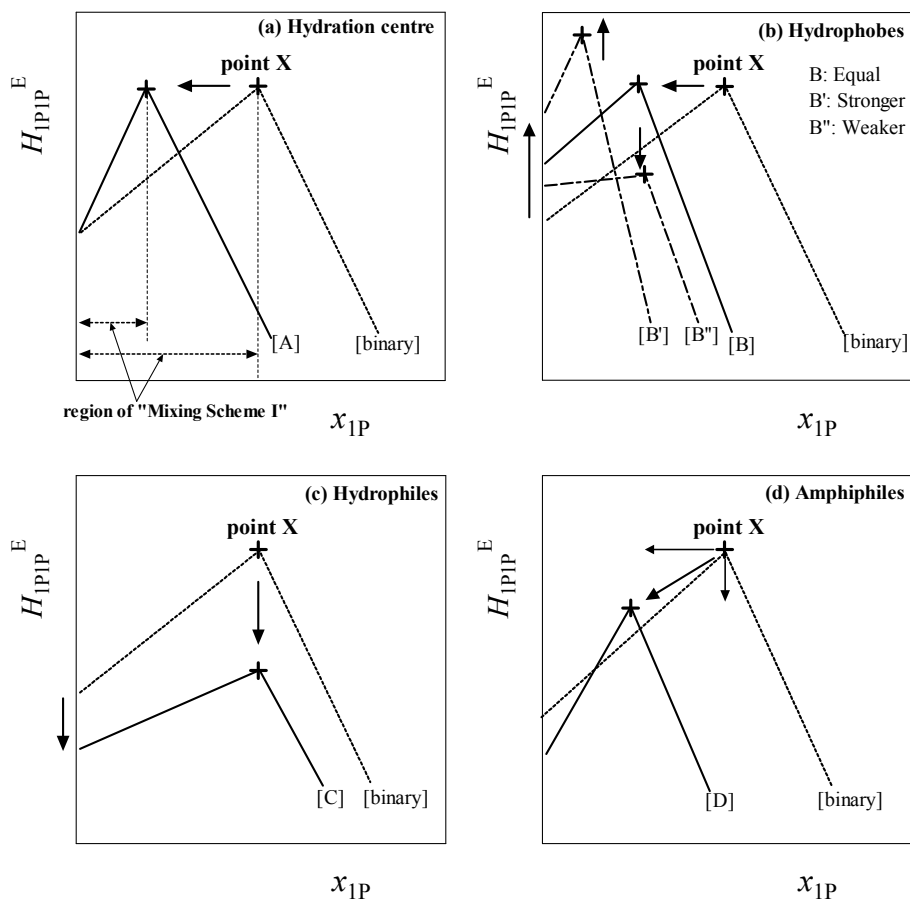


Figure 2 Induced changes of  $H_{1P|1P}^E$  pattern in the presence of various types of solute S. [Binary] represents the binary 1P-H<sub>2</sub>O system without test solute S. (a) Effects of the hydration centre on the pattern per unit increase in test sample S. Region of Mixing Scheme I is defined as  $x_{1P} = 0$  to  $x_{1P}$  at point X, as described on the horizontal axis, (b) the effects of hydrophobes, (c) hydrophiles and (d) amphiphiles.

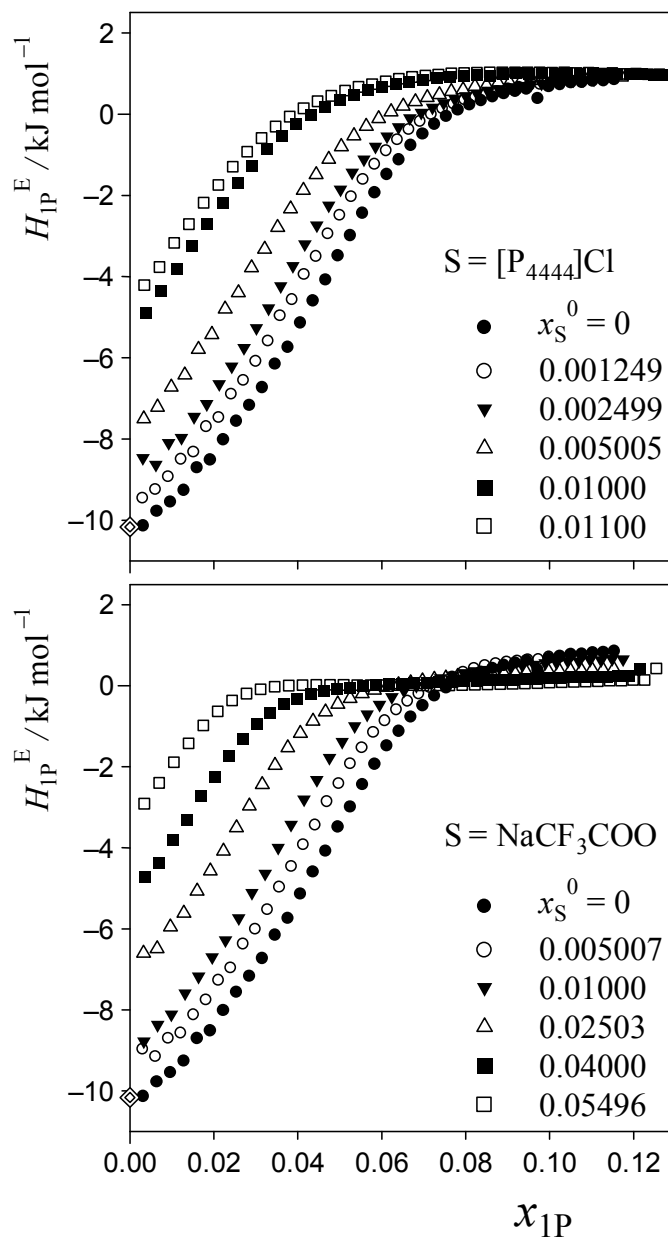


Figure 3 Excess partial molar enthalpy,  $H_{1P}^E$ , of 1P in 1P-S-H<sub>2</sub>O at 25 °C and given initial salt concentration,  $x_S^0$ . Diamonds represent  $H_{1P}^E$  in dilute solution, as reported by Wadso *et al.*<sup>35</sup>

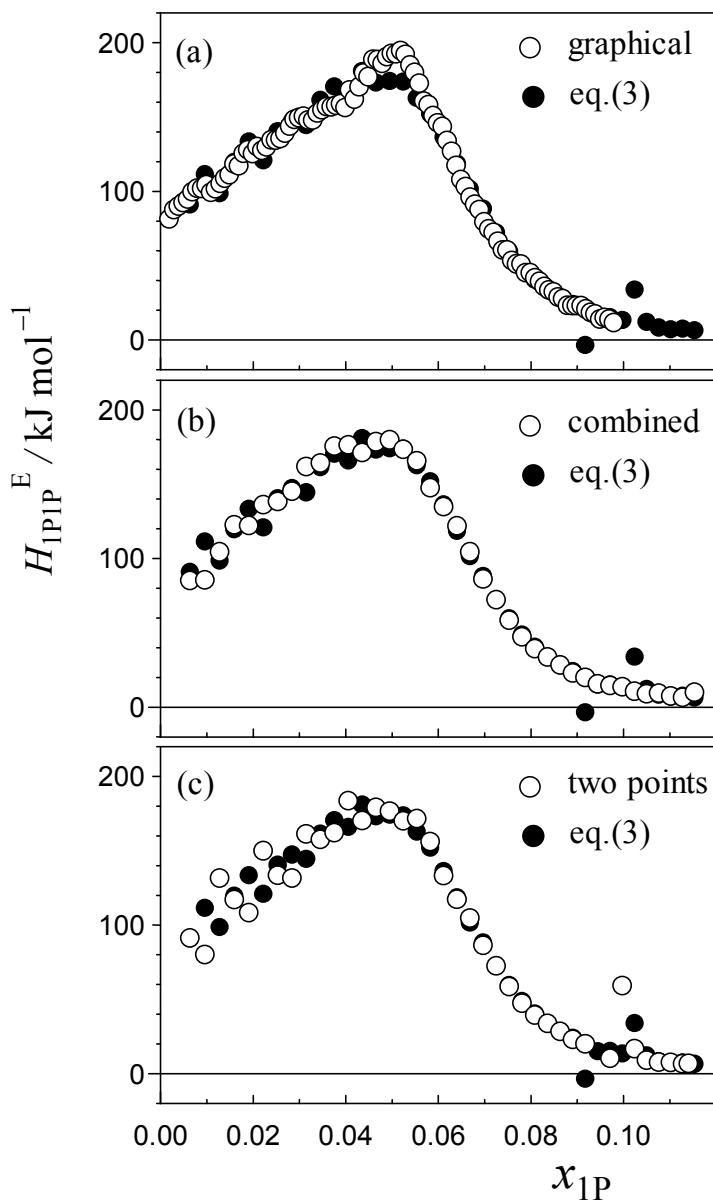


Figure 4 Comparison of  $H_{IPIP}^E$  pattern for the binary (1-propanol–H<sub>2</sub>O) mixture calculated based on differentiation using Eq. (3) (solid circles) with those using other evaluation methods (open circles); (a) typical graphical evaluation normally exercised for 1P-probing studies,<sup>34</sup> (b) combination of calculation using Eq. (3) and graphical evaluation, (c) simple derivative using two data points with  $\delta x_{1P} \approx 0.006$ .

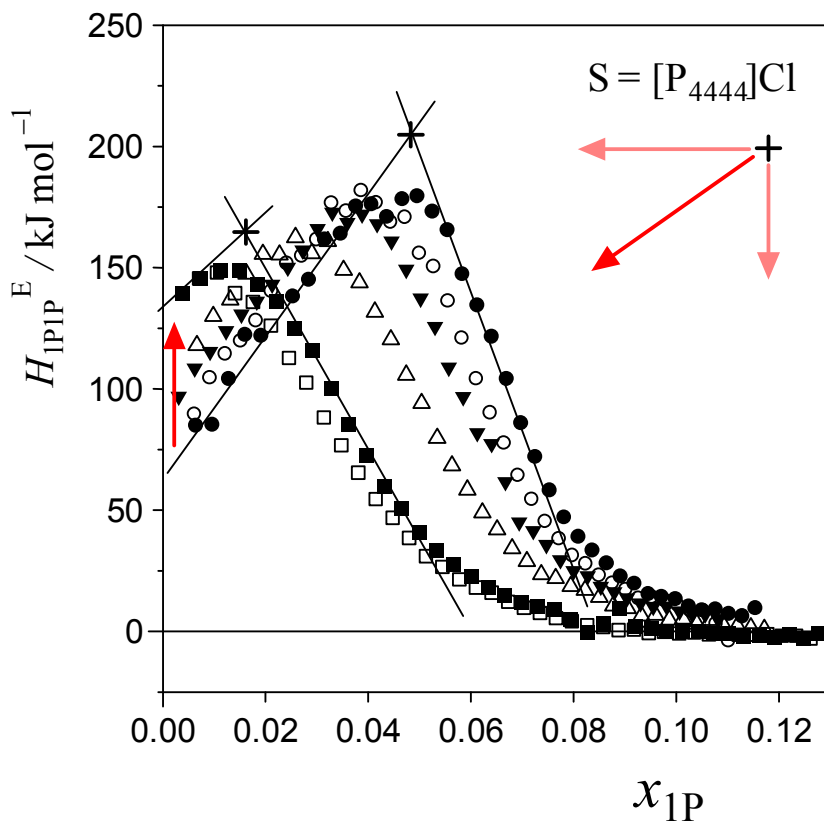


Figure 5 Enthalpic 1P–1P interaction,  $H_{1P1P}^E$ , of 1P–[P<sub>4444</sub>]Cl–H<sub>2</sub>O at 25 °C for given initial salt concentrations,  $x_S^0$ . The initial concentrations,  $x_S^0$ , were set at 0, 0.001249, 0.002499, 0.005005, 0.01000 and 0.01100 from right to left in the figure. Mixing Scheme I is classified from  $x_{1P} = 0$  to  $x_{1P}$  at point X. The region decreases with increasing  $x_S^0$  and nearly disappears at  $x_S^0 \approx 0.011$ . Point X is largely compressed in the westward and southward directions.

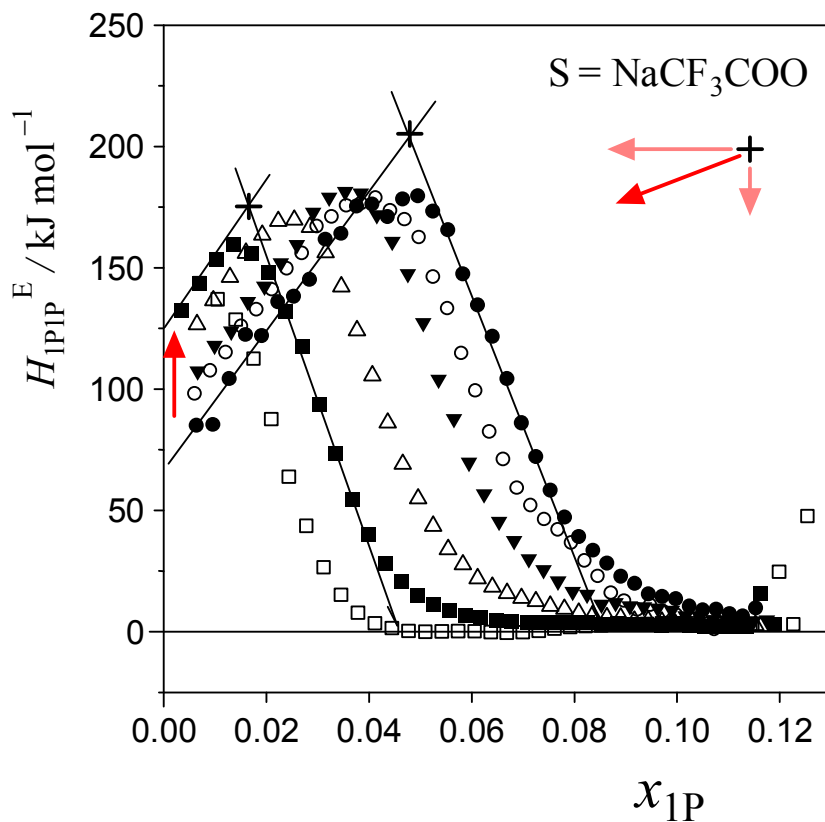


Figure 6 Enthalpic 1P–1P interaction,  $H_{1P1P}^E$ , of 1P– $\text{NaCF}_3\text{COO}$ – $\text{H}_2\text{O}$  at 25 °C for given initial salt concentrations,  $x_S^0$ . The initial concentrations,  $x_S^0$ , were set at 0, 0.005007, 0.01000, 0.02503, 0.04000 and 0.05496 from right to left in the figure. Mixing Scheme I decreases with increasing  $x_S^0$  and disappears around  $x_S^0 \approx 0.055$ . Point X is compressed mainly in the westward direction.

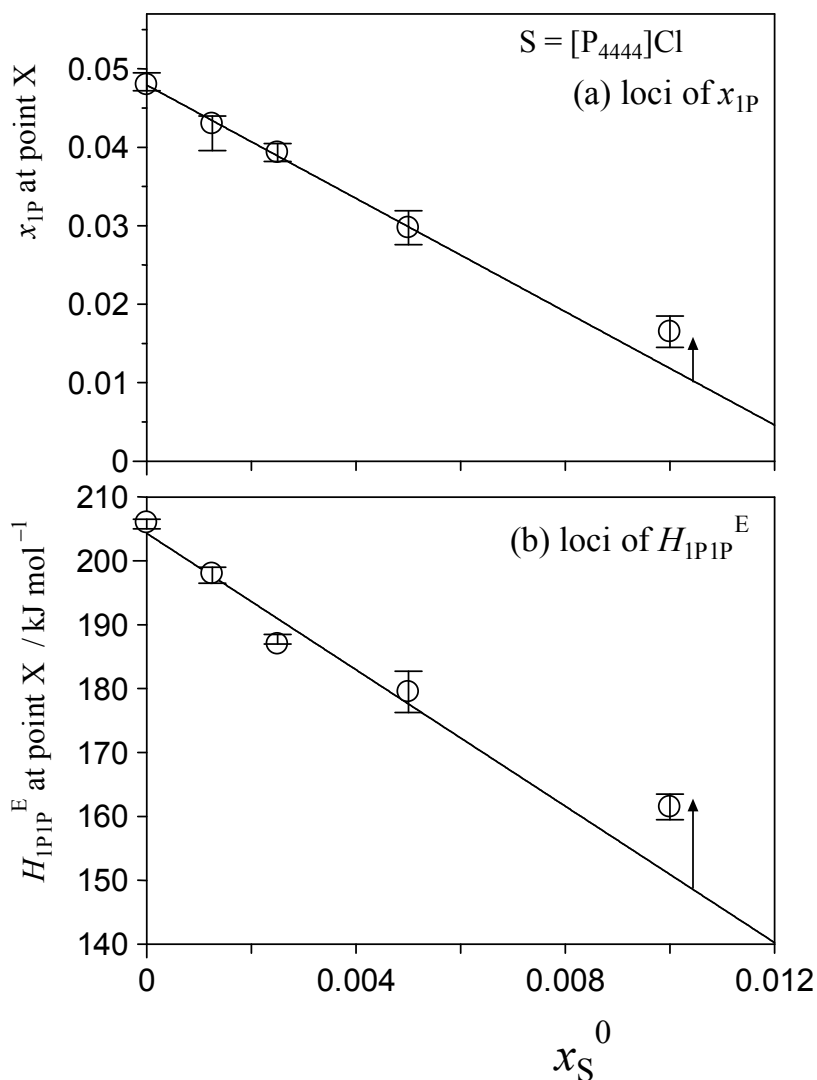


Figure 7 Loci of point X as a function of the initial salt concentration,  $x_S^0$ , for  $S = [P_{4444}]Cl$ . (a) The loci of  $x_{IP}$  at 25 °C. The slope gives the hydrophobicity index and hydration number,  $n_H$ . These parameters were evaluated from the slope following subtraction of the  $Cl^-$  counterion contribution. (b) The loci of  $H_{IPIP}^E$  at 25 °C. The slope corresponds to the hydrophilicity index, as  $Cl^-$  is classified as the hydration centre. The hydrophilicity index of  $Cl^-$  is zero.

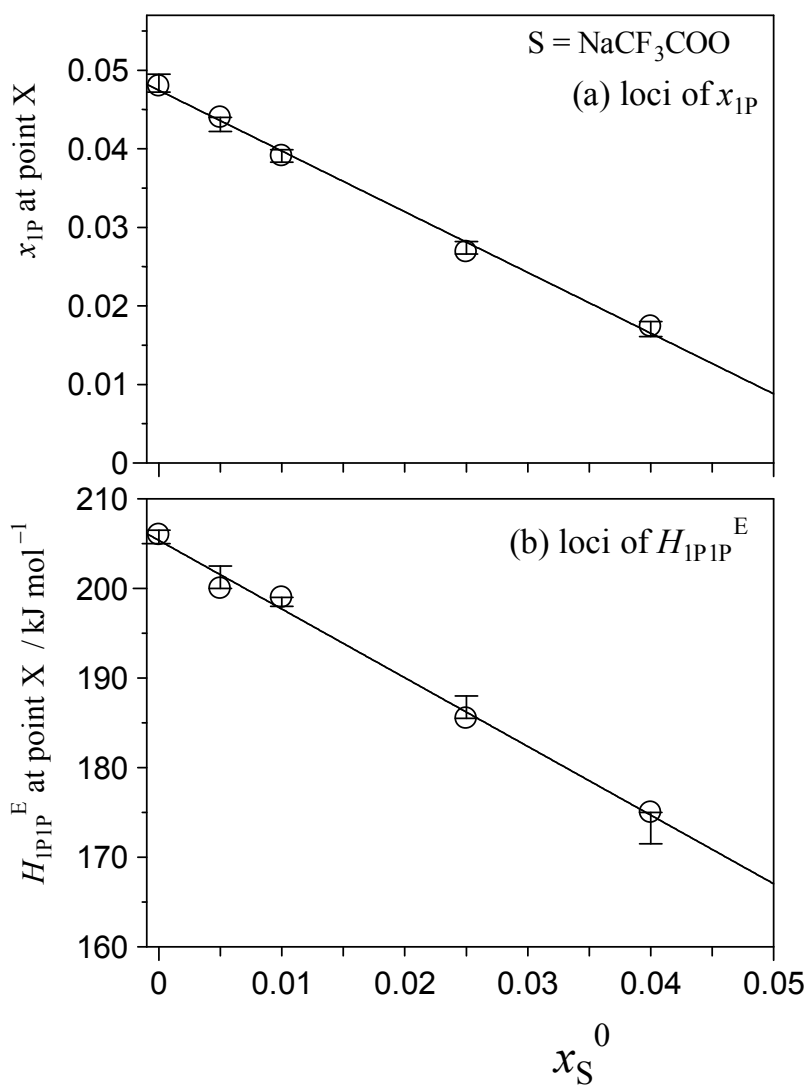


Figure 8 Loci of point X as a function of initial salt concentration,  $x_S^0$ , for  $S = \text{NaCF}_3\text{COO}$ . (a) The loci of  $x_{1P}$  at 25 °C. The slopes give the hydrophobicity index and hydration number,  $n_H$ . These parameters were evaluated from the slope following subtraction of the  $\text{Na}^+$  counterion contribution. (b) The loci of  $H_{1P1P}^E$  at 25 °C. The slope corresponds to the hydrophilicity index, as  $\text{Na}^+$  is classified as the hydration centre. The hydrophilicity index of  $\text{Na}^+$  is zero.

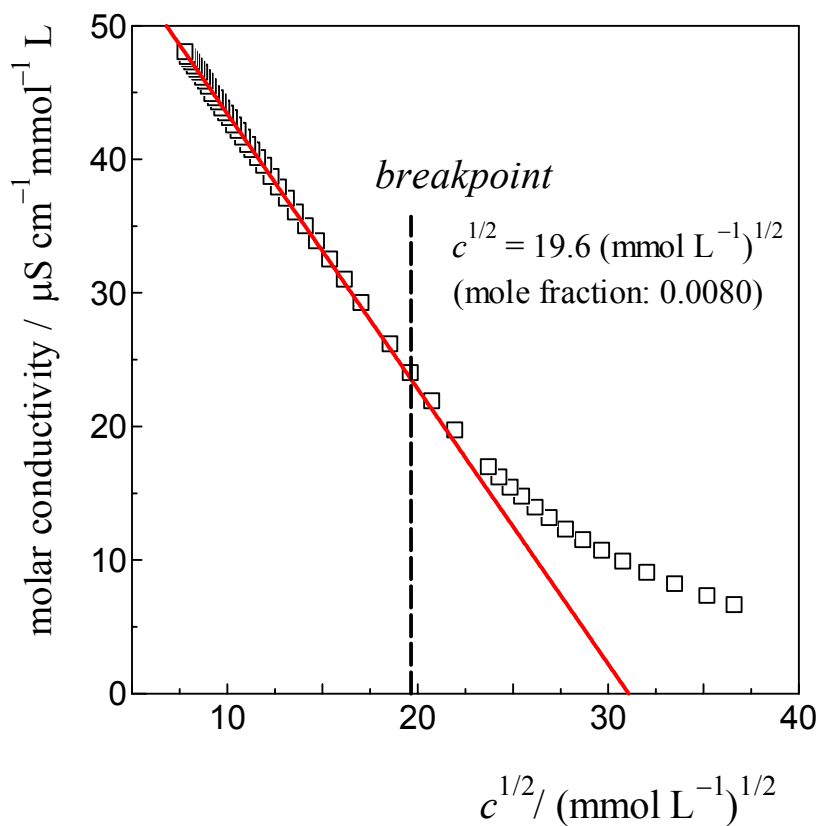


Figure 9 The isotherm of electric conductivity for aqueous solutions of [P<sub>4444</sub>]CF<sub>3</sub>COO based on the Kohlrausch empirical relation.<sup>42</sup> The breakpoint was estimated to be  $c^{1/2} = 19.6 (\text{mmol} \cdot \text{L}^{-1})^{1/2}$  for [P<sub>4444</sub>]CF<sub>3</sub>COO, corresponding to a 0.0080 mole fraction of the IL.

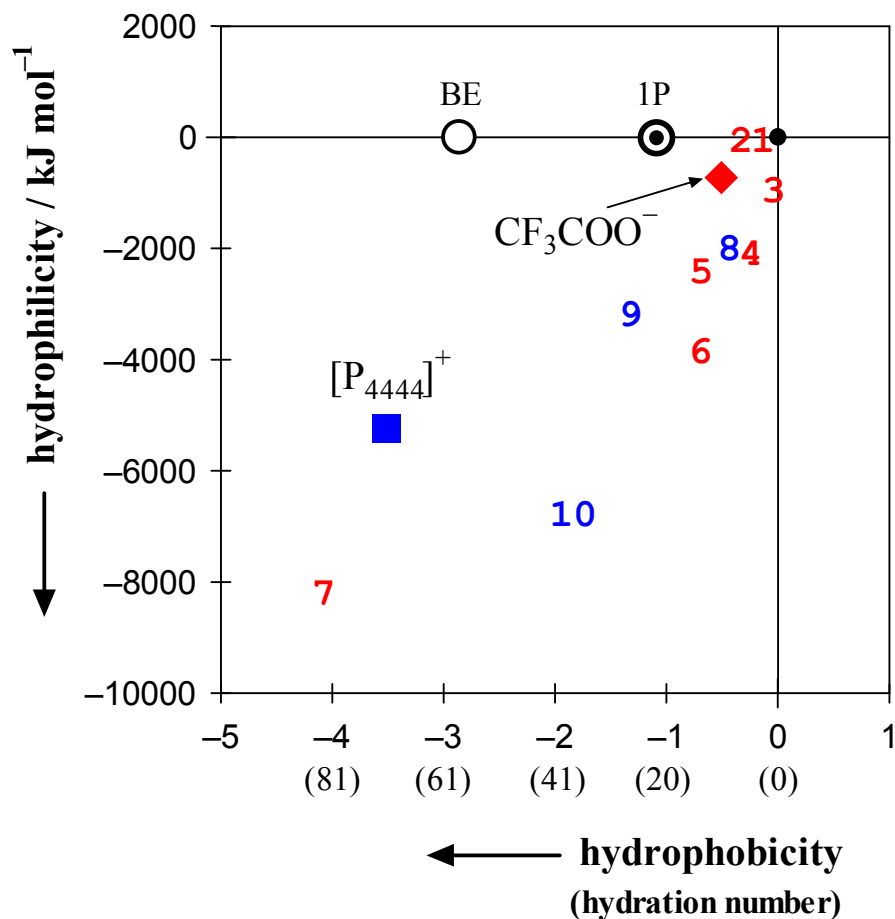


Figure 10 2D map of hydrophobicity/hydrophilicity for typical constituent ions of ionic liquids. Values in parentheses on the horizontal axis denote hydration numbers. H<sub>2</sub>O is located at the origin (0,0) and the probing 1P is located at (-1,0). The square and the diamond represent the present results for [P<sub>4444</sub>]<sup>+</sup> and CF<sub>3</sub>COO<sup>-</sup>, respectively. Seven other constituent anions<sup>20,21,30</sup> and three cations<sup>20,21</sup> are shown together; 1: Cl<sup>-</sup>, 2: CH<sub>3</sub>COO<sup>-</sup>, 3: Br<sup>-</sup>, 4: BF<sub>4</sub><sup>-</sup>, 5: [OTf]<sup>-</sup>, 6: PF<sub>6</sub><sup>-</sup>, 7: [NTf<sub>2</sub>]<sup>-</sup>, 8: [C<sub>2</sub>mim]<sup>+</sup>, 9: [C<sub>4</sub>mim]<sup>+</sup>, 10: [C<sub>4</sub>C<sub>1</sub>mim]<sup>+</sup>. An aqueous solution of 2-butoxyethanol (abbreviated as BE) exhibits an LCST below 50 °C.<sup>50,51</sup> See text for discussion.